Journal of Applied Physics

Self-regulating plasma-assisted growth of epitaxial $BaBiO_3$ thin-film on $SrTiO_3$-buffered Si(001) substrate

Cite as: J. Appl. Phys. **132**, 225304 (2022); https://doi.org/10.1063/5.0101227
Submitted: 07 June 2022 • Accepted: 17 November 2022 • Published Online: 09 December 2022

I. Ahmed, S. De Gendt and C. Merckling

AIP Publishing

Journal of Applied Physics ARTICLE scitation.org/journal/jap

Self-regulating plasma-assisted growth of epitaxial $BaBiO_3$ thin-film on $SrTiO_3$-buffered Si(001) substrate

Cite as: J. Appl. Phys. **132**, 225304 (2022); doi: 10.1063/5.0101227
Submitted: 7 June 2022 · Accepted: 17 November 2022 ·
Published Online: 9 December 2022

I. Ahmed,[1,2,a)] S. De Gendt,[2,3] and C. Merckling[1,2]

AFFILIATIONS

[1]Department of Materials Engineering, KU Leuven, Kasteelpark Arenberg 44, 3001 Leuven, Belgium
[2]Imec, Kapeldreef 75, 3001 Leuven, Belgium
[3]Department of Chemistry, KU Leuven, Celestijnenlaan 200F, 3001 Leuven, Belgium

[a)]**Author to whom correspondence should be addressed:** islam.ahmed@imec.be

ABSTRACT

The $BaBiO_3$ perovskite oxide is an interesting material system because of its superconductivity when p-doped and the predicted topological insulating nature when n-doped. Single crystalline $BaBiO_3$ films are grown by molecular beam epitaxy with high quality utilizing the adsorption-controlled regime, where volatile Bi is supplied in excess in the presence of oxygen radicals. $BaBiO_3$ films are integrated on Si(001) substrates through growth on a $SrTiO_3$(001) buffer layer. Despite the 11.77% lattice mismatch, by systematically varying growth parameters, such as plasma conditions, substrate temperature, and metallic fluxes, a growth window for the $BaBiO_3$ is well-established. Within the optimum growth window, films are stoichiometric and of high crystalline quality based on the different physical characterization techniques. The development of robust layers is facilitated by accessing the self-regulating regime, where only the stoichiometric quantity of Bi sticks during the epitaxy.

I. INTRODUCTION

Topological insulators have insulating bulk alongside robust conductive surface states, expressed by Dirac-dispersion in the bulk bandgap. Bi-containing compounds possess a strong spin–orbit coupling (SOC) for *6s* and *6p* electrons of bismuth, which are fundamental interactions for the manifestation of topological insulating properties. $Bi_{1-x}Sb_x$, Bi_2Se_3, and Bi_2Te_3 already were discovered as 3D topological insulators driving technological advances in spintronics, quantum technology, and thermoelectrics.[1,2] Therefore, exploration of new material families with non-trivial topology has become a main research focus for theoretical and experimental physicists. Recently, density-functional theory (DFT) studies, with Bi's SOC considered, show induced topologically protected surface states with a band inversion between Bi-*6s* states and Bi-*6p* in electron doped $BaBiO_3$ (BBO).[3] If experimentally realized, BBO will be the compound with a TI bandgap of 0.7 eV, the largest along all known with natural stability against surface oxidation.

Since their emergence as high-T_c superconducting oxides, Bi-based perovskites $BaPb_xBi_{1-x}O_3$[4] and $Ba_{1-x}M_xBiO_3$ (with M = K or Rb[5,6]) attracted wide research interest. Three-dimensional crystals, such as $BaPb_{0.3}Bi_{0.7}O_3$ and $Ba_{0.6}K_{0.4}BiO_3$ (BKBO), are superconducting with a critical temperature of 13 and 29.8 K, respectively. The low density of charge at the Fermi level of the structurally undistorted perovskites raised ambiguity related to their superconducting behavior, contradicting well-established understanding for superconductivity in metals,[7] especially due to the absence of magnetic ordering.[8] The mechanism for peculiar superconductivity was later attributed to the parent BBO unconventional insulating nature. BKBO/BBO/BKBO with high quality barriers can be used in superconductor–insulator–superconductor based devices and superconducting circuits.[9] Additionally, the superconducting hole doped BBO and the TI electron doped BBO is predicted to be a host solid state system for the proximity effect based exotic Majorana bound states.[10] The two doped layers are brought in close contact as a device concept for developing a

topological qubit. All this requires high control over dopant profiles and interface quality during the epitaxy of the heterostructure.

Crystalline materials provide a wide playground for solid state explorations especially when short range interactions take place in the heterostructure. Molecular beam epitaxy (MBE) allows for high controllability on the crystalline quality and phase purity. MBE has been routinely used as a low energetic deposition technique to grow epitaxial thin-films. Yet, the stoichiometry control of the compound deposited can still be challenging. One approach to access the self-regulating regime is to grow layers utilizing hybrid-MBE, where a volatile component is introduced to the growth surface as a metal–organic precursor as demonstrated for the successful growth of stoichiometric $SrVO_3$, $SrTiO_3$ (STO), and $BaTiO_3$ layers with high crystalline quality.[11–13]

Thin-films of BBO have been previously grown by different techniques, such as pulsed laser deposition (PLD),[14,15] sputtering methods,[16] and MBE.[17–19] Available commercial oxide substrates are STO with lattice constant $a_{STO} = 3.905$ Å and MgO with $a_{MgO} = 4.212$ Å. BBO with a pseudo-cubic lattice constant of $a_{BBO} = 4.365$ Å has been epitaxially deposited on both substrates despite the lattice mismatch f of 11.77% and 3.63%, respectively. Typically, film's out-of-plane orientation follows that of the underlying substrate's lattice. However, the previous study shows pre-dominantly (110)-BBO when grown by MBE on an STO(001) substrate, while a 2 nm BaO buffer layer helps in stabilizing BBO(001) films instead.[20] A (110)-oriented BBO film was also observed for films grown on an MgO substrate by MBE despite the smaller lattice mismatch.[21] Attempts to grow BBO directly on Si substrates by PLD resulted in non-epitaxial but textured thin-films.[22] In this paper, we report on the growth of single crystalline BBO thin-films by MBE on an Si substrate, utilizing the technique developed by McKee *et al.*[23] A commensurate STO(001) buffer layer is grown epitaxially on Si(001) to help in investigating the mechanism of bismuthate epitaxy. The grown layers will be used later on as a platform to investigate the transport and other intrinsic material characteristics.

II. EXPERIMENTAL

BBO/STO/Si(001) heterostructures are grown using a Riber 49 MBE reactor at a base pressure of 1×10^{-10} Torr. Strontium, barium, and bismuth are evaporated by dual-filament thermal effusion cells, while titanium is evaporated by an electron beam and controlled by a feedback loop with a mass spectrometer to keep a constant Ti flux during STO growth.[24] *In situ* quartz crystal microbalance (QCM) is utilized to calibrate independently the adequate flux of each metallic beam. The flux ratio is varied from 1:1 to 5.7:1 to investigate the sticking coefficient behavior of both barium and bismuth. Molecular oxygen is introduced to the growth chamber through a remote radio-frequency (RF) plasma source controlled by a mass-flow controller to inject either molecular or atomic oxygen gas. Monitoring the wafer surface temperature during epitaxy is carried out by a calibrated optical pyrometer. Prior to the growth, the Si wafer is dipped into a 2% HF solution for 90 s to remove the native SiO_2 and other organic contaminants.

Growth mode and film morphology are monitored by the real-time *in situ* reflection high-energy electron diffraction (RHEED) utilizing an e-gun operating at 20 kV. The growth of complex oxides on silicon is facilitated by the ability to grow an epitaxial STO (001) single crystalline buffer layer with a 45° lattice rotation ($\langle 100\rangle_{STO(001)} \| \langle 110\rangle_{Si(001)}$) with the aid of a fully commensurate half monolayer of Sr to avoid the thermodynamic instability between STO and Si[23] before introducing oxygen. The lattice rotation will ensure the commensurate growth of the STO(001) template on the Si(001) surface with a reduced effective lattice mismatch of only 1.7%.[25] The same recipe for the 15-nm-thick STO/Si pseudo-substrates was used throughout the BBO growth experiments to reduce quality fluctuations among the different virtual substrates.[26,27]

Structural perfection and phase purity of the films are investigated with high-resolution x-ray diffraction (HR-XRD, PANalytical's Material Research tool). ω–2θ XRD logarithmic plots are collected between $18° \leq \omega \leq 35.2°$ using Cu $K_{\alpha 1}$ radiation line ($\lambda \approx 0.154$ nm). Out-of-plane lattice parameters are calculated based on the peak positions of both BBO and STO layers in the symmetric scans according to Bragg's law. Full width at half-maximum (FWHM) of the STO buffer layers' rocking curves (RCs) is calculated to be below 0.4° for all substrates denoting their robustness as good templates for BBO growth. The characterization of BBO surface roughness is carried out in a Bruker dimension edge atomic force microscope (AFM) operating in a tapping mode. For composition analysis, Rutherford backscattering spectroscopy (RBS) is utilized to measure the Bi/(Bi + Ba) stoichiometry of the BBO epitaxial layers.

III. RESULTS

Figure 1(a) presents the symmetric out-of-plane wide range ω–2θ XRD scans for the heterostructures grown with different O_2 plasma power conditions. The XRD spectra of different films are normalized relative to the Si(004) Bragg diffraction peak at $\omega = 34.56°$. Diffraction peaks centered around $\omega = 23.15°$ correspond to the STO(002) reflection, denoting stable and high crystalline quality of the virtual substrate with a cubic lattice constant of 3.917 Å. The BBO(002) peak is centered around $\omega = 20.62°$, corresponding to an out-of-plane lattice parameter of 4.376 Å for the pseudo-cubic structure. BBO(002) XRD diffraction peaks are only observed for a plasma power of 450 W and higher. It is important to notice that the typical breathing and tilt distortions for BBO are not significant enough for XRD to resolve them; therefore, a pseudo-cubic lattice parameter is assigned to the grown thin-films. In Fig. 1(b), the chemical composition of the thin-films as studied by RBS is shown. Film grown at a high plasma power of 600 W becomes stoichiometric with Bi/Bi + Ba = 0.5, along higher crystallinity as reflected in the intense Bragg diffraction peak. However, lower intensity of the BBO diffraction peak upon using 450 W depicts that the degree of crystallinity seems to be directly correlated to the Bi concentration in the perovskite thin-film. As seen for XRD scans done on films grown at plasma conditions of 0, 150, and 300 W, the effect is even more pronounced with the complete extinction of the BBO diffraction peak in the films where the composition is more than 25% off-stoichiometry.

To determine the optimal growth conditions for BBO, the substrate temperature window is also mapped out at 600 W. As illustrated in Figs. 2(a) and 2(b), in the high temperature regime (>650 °C), films are more than 25% off-stoichiometry, hence hardly resulting in a diffraction peak from BBO(002). On the other hand,

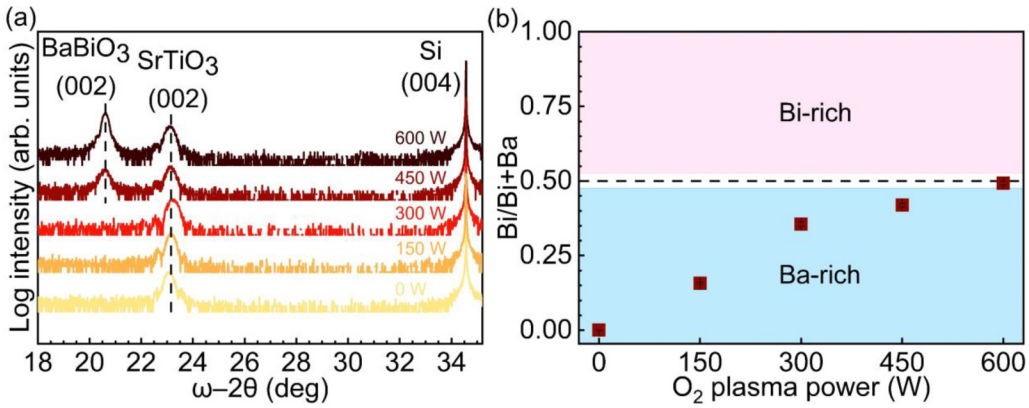

FIG. 1. BBO thin-films grown at different O_2 plasma conditions between 0 and 600 W with a step of 150 W, while the substrate temperature is fixed at 600 °C: (a) wide range ω–2θ scans of Si substrate, STO buffer layer, and BBO diffraction peaks and (b) stoichiometry evolution with plasma conditions of the thin-films as measured by RBS.

for temperatures ranging from 450 to 650 °C, diffraction peaks of BBO(002) are clearly observed. However, variation among quality of films can be noticed based on the individual FWHM of ω–scans around the BBO(002) diffraction peaks, which reflects the layer's mosaic spread in the out-of-plane direction, as shown in Fig. 2(c). It can be observed that both crystalline perfection and film quality are relatively much enhanced at 600 °C (FWHM = 0.55°), indicating that quality of the layer is only limited by the crystal quality of the underlying STO buffer (with FWHM = 0.34°, in this case). Films grown at 550 °C contain two different out-of-plane crystallographic

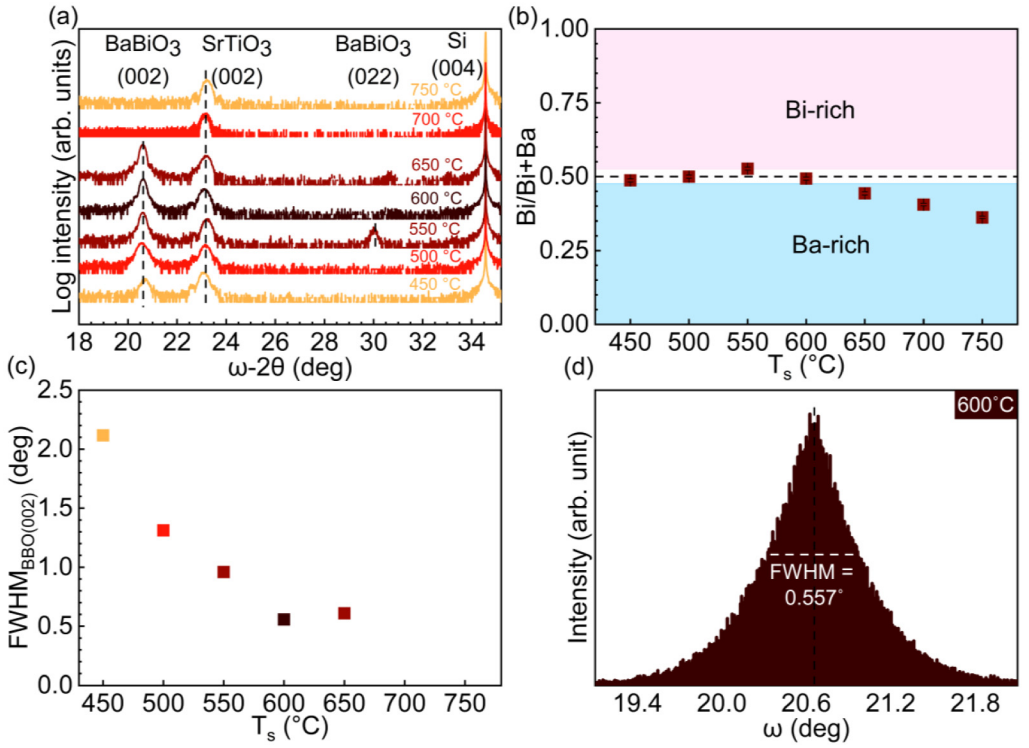

FIG. 2. BBO thin-films grown at different substrate temperatures (T_s) with plasma conditions of 600 W: (a) wide range ω–2θ scans of the heterostructures, (b) stoichiometry of the thin-films measured by RBS, and (c) FWHM of the grown thin-films with the (d) RC for the highest quality film, highlighting the quality of the film grown at 600 °C.

orientations, with an additional peak centered around ω = 30.03° besides the typical (002) peak for BBO, which is further discussed in Sec. IV.

IV. DISCUSSION

RBS data of Fig. S1 in the supplementary material depict the insensitivity of Ba content in the films to either plasma conditions or substrate temperature. This suggests a sticking coefficient of unity for Ba, as was previously reported by Hellman *et al.*[17]. Meaning that once Ba is oxidized and incorporated into the film, it does not desorb, even not at the high temperature regime (>650 °C). Contrary to Ba, the Bi (group V element) incorporation at an elevated temperature seems to be particularly challenging for thin-film growth by MBE, mainly due to the volatility of Bi.[28–30] Bi content is highly dependent on plasma oxidation power. Epitaxy of stoichiometric BBO only takes place when enough energetic oxygen radicals are provided at the growth surface. Two possible mechanisms are proposed (1) to ensure complete oxidation of Bi by energetic radicals and (2) the cracking of Bi dimers,[31] which are evaporated from the Knudsen cell, hence helping in the direct incorporation of Bi atoms into energetically favorable sites. Plasma provides the necessary conditions for the chemical reaction at the growing oxide surface by generating highly reactive oxygen species, which can be directly incorporated into the lattice.[32] Activated oxygen helps in the breakdown of other species reaching the surface into more mobile adatoms, more readily oxidized and incorporated,[25] especially that Bi in the oxidized form has lower vapor pressure than its elemental form.[33] Plasma oxygen plays the same role ozone does for $PbTiO_3$ by driving the stability line of solid phase formation of the oxide lower and readily incorporate the volatile element in the film.[34] Therefore, using plasma oxygen is a key parameter for growing BBO by supporting the nucleation and growth of the film. The lower intensity of the BBO(002) diffraction peak and the film quality at low temperatures (450 °C) in Fig. 2(a) are not precisely linked to the content of Bi in the film. Since Bi vapor pressure is relatively within the same range at 600 °C and a lower growth temperature,[35] it could be a matter of the activation energy needed for the crystal formation and adatoms mobility, which vary exponentially with the growth temperature. Furthermore, the additional diffraction peak arising at 550 °C centered around ω = 30.03° is assigned to the presence of a different film orientation BBO(110). Understanding about the driving force behind the formation of this orientation is still missing.

To further study the growth regime, one metallic flux is fixed and the other is varied, while the reaction kinetics are closely

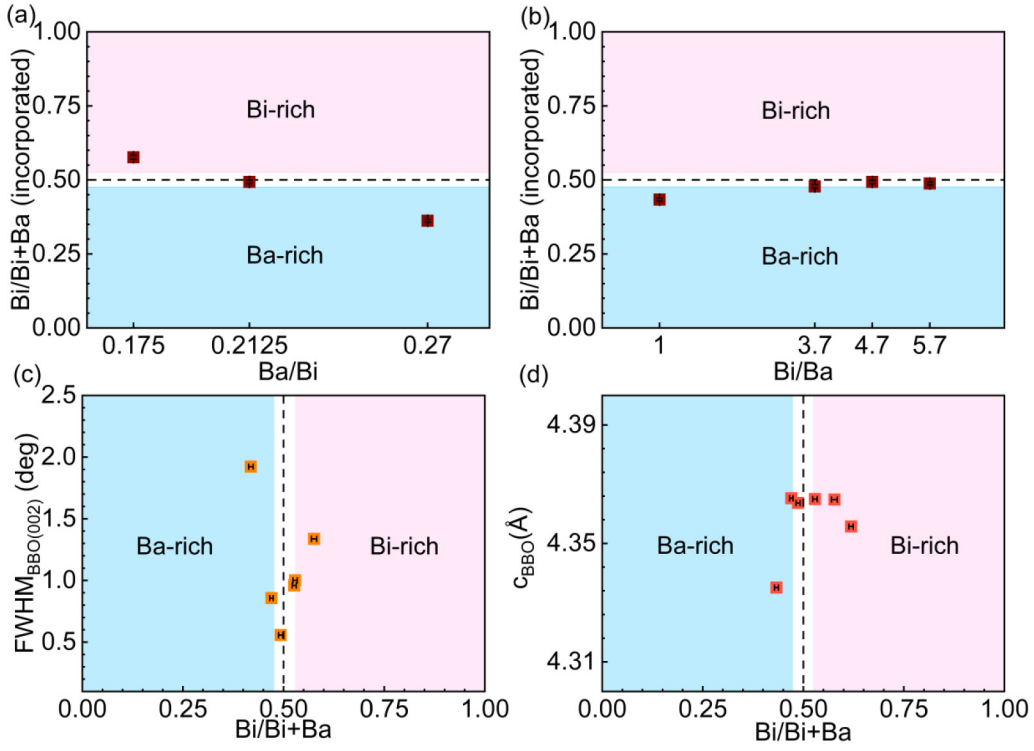

FIG. 3. RBS stoichiometry for $BaBiO_3$ films grown at 600 °C and 600 W plasma power (a) grown at different Ba fluxes of (1.4, 1.7, and 2.16 A/s) while keeping the Bi flux constant at 8 A/s, hence the Ba/Bi flux ratio of 0.175, 0.2125, and 0.27, respectively, (b) at different Bi fluxes of (1.7, 6.3, 8, and 9.7 A/s) while keeping the Ba flux constant at 1.7 A/s, hence the Bi/Ba flux ratio of 1, 3.7, 4.7, and 5.7, respectively. (c) FWHM of layers with different compositions and (d) out-of-plane lattice parameters extracted for films grown within and around the growth window.

investigated. Agreeing with the previous XPS study,[36] Bi incorporation is found to be inversely proportional to the amount of incorporated Ba according to Fig. 3(a). The film is becoming Ba-rich by increasing the flux of barium incident on the surface while keeping bismuth flux fixed. In Fig. 3(c), films deviating from ideal stoichiometry are of lower crystalline quality reflected from their FWHM higher values. To access full controllability over the self-regulated growth facilitated by the volatile Bi, the growth rate must be carefully chosen by controlling Ba flux; that is why a barium flux of 1.7 A/s is chosen. As illustrated in Fig. 3(b), beyond a certain flux of Bi incident on the substrate, the growth is barely Bi flux dependent, which is an ultimate signature for adsorption-controlled growth,[30] where only the proper amount of BiO is incorporated for the $BaBiO_3$ crystal synthesis. This is similar to other complex oxides grown by hybrid-MBE and GaAs crystal growth where just the necessary amount of As atoms stick to respect the III:V stoichiometry.[37] A certain overpressure of Bi flux is still required besides the high oxidation capability of the provided plasma. This allows for the growth of stoichiometric films within a growth window with no dependence of the flux ratio. The extracted lattice parameters within this growth window are almost constant and independent of the flux ratio; however, there is a deviation from the ideal pseudo-cubic lattice parameter of BBO of up to −1.05% outside the growth window observed, as shown in Fig. 3(d).

The RHEED pattern recorded along ⟨110⟩ azimuth is shown in Fig. 4(b) for stoichiometric BBO grown at 600 °C. The streaky pattern denotes layer-by-layer growth and smooth surface. Faint intensity streaks can also be noticed in between the main streaks, which corresponds to a sixfold surface reconstruction along ⟨110⟩. In Fig. 4(a), the superimposed diffraction pattern of additional spots on the typical streaks suggests that (110) faceting occurs in addition to the smooth (001) surface, consistent with the additional XRD diffraction peak showing up at ω = 30.03° for the film grown at 550 °C. Based on these observations, RHEED can be utilized as *in situ* characterization of the growth window of BBO. For surface morphology, the AFM image in Fig. 4(f) of ≈22 nm thick BBO shows low surface roughness with the RMS-value below 2.5 Å, hence the absence of secondary phases within the BBO layer. Smoothness of films within the growth window is a proof of a layer-by-layer growth mechanism. Contrary to the thin-film grown at 550 °C where 3D islands with an average height of 20 nm are grown out of the smooth surface [shown in Fig. 4(d), which is attributed to the additional film orientation].

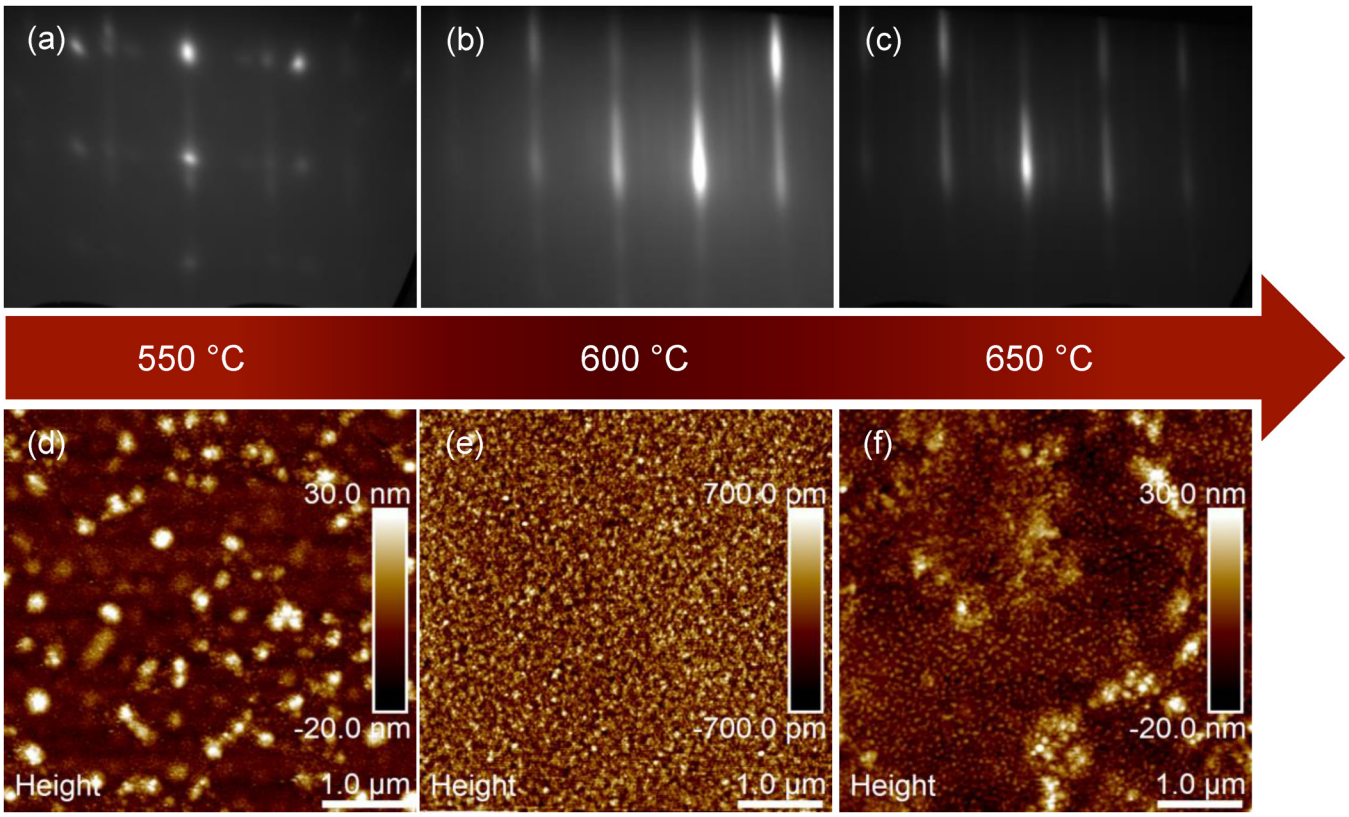

FIG. 4. RHEED patterns for films grown with the same flux ratio and the O_2 plasma power of 600 W at different T_s: (a) 550, (b) 600, and (c) 650 °C. AFM images for thin-films grown at 600 W with T_s of (d) 550, (e) 600, and (f) 650 °C. AFM z-height scale bars in nm and pm are shown on the right for each image.

V. CONCLUSIONS

In this study, we shed light on the MBE growth mechanism of bismuthate perovskite. BBO growth conditions are well investigated by analyzing the film crystal perfection, epitaxial quality, and morphology using RHEED, XRD, AFM, and RBS. The growth window is mapped in terms of substrate temperature, plasma conditions, and flux ratio based on the quality and lattice parameters of the MBE grown layers. Carefully choosing the plasma conditions is a crucial step toward realizing high quality BBO thin-films. The absence of multi-phases within the film and its smoothness is a proof of accessing a self-regulated growth regime, which is cross-checked by XRD crystalline quality and film composition. Crystalline BBO films are grown on an STO(001)/Si virtual substrate for the first time with high quality, which is only limited by the quality of the underlying substrate. Like other compounds containing a group-V element, BBO perovskite synthesis follows the adsorption-controlled regime within which high quality stoichiometric layers can be developed allowed using oxygen radicals via conventional-MBE.

SUPPLEMENTARY MATERIAL

See the supplementary material that includes data showing the direct effect of plasma oxygen and substrate temperature on the incorporation of bismuth and barium separately based on RBS data.

ACKNOWLEDGMENTS

The authors would like to thank process and hardware engineers: Hans Costermans and Kevin Dubois for their great support on the MBE cluster tool, as well as Johan Desmet and Johan Meersschaut for RBS operations and data analysis. This research has received funding from the European Research Council (ERC) under the European Union's Horizon 2020 research and innovation program (Grant Agreement No. 864483).

AUTHOR DECLARATIONS

Conflict of Interest

The authors have no conflicts to disclose.

Author Contributions

I. Ahmed: Data curation (lead); Formal analysis (lead); Writing – original draft (lead). **S. De Gendt:** Validation (supporting); Writing – review & editing (supporting). **C. Merckling:** Funding acquisition (lead); Investigation (lead); Project administration (lead); Supervision (lead); Writing – review & editing (supporting).

DATA AVAILABILITY

The data that support the findings of this study are available from the corresponding author upon reasonable request.

REFERENCES

[1]H. Zhang, C. X. Liu, X. L. Qi, X. Dai, Z. Fang, and S. C. Zhang, "Topological insulators in Bi_2Se_3, Bi_2Te_3 and Sb_2Te_3 with a single Dirac cone on the surface," Nat. Phys. **5**(6), 438–442 (2009).
[2]A. A. Taskin and Y. Ando, "Quantum oscillations in a topological insulator $Bi_{1-x}Sb_x$," Phys. Rev. B **80**(8), 085303 (2009).
[3]B. Yan, M. Jansen, and C. Felser, "A large-energy-gap oxide topological insulator based on the superconductor $BaBiO_3$," Nat. Phys. **9**(11), 709–711 (2013).
[4]A. W. Sleight, J. L. Gillson, and P. E. Bierstedt, "High-temperature superconductivity in the $BaPb_{1-x}Bi_xO_3$ system," Solid State Commun. **88**(11–12), 841–842 (1993).
[5]L. F. Mattheiss, E. M. Gyorgy, and D. W. Johnson, Jr, "Superconductivity above 20 K in the Ba-K-Bi-O system," Phys. Rev. B **37**(7), 3745 (1988).
[6]S. Tajima, S. Uchida, A. Masaki, H. Takagi, K. Kitazawa, S. Tanaka, and A. Katsui, "Optical study of the metal-semiconductor transition in $BaPb_{1-x}Bi_xO_3$," Phys. Rev. B **32**(10), 6302 (1985).
[7]J. B. Boyce, F. G. Bridges, T. Claeson, T. H. Geballe, and J. M. Remeika, "X-ray absorption of $BaBiO_3$ and superconducting $BaBi_{0.25}Pb_{0.75}O_3$," Phys. Rev. B **41**(10), 6306 (1990).
[8]Y. J. Uemura, B. J. Sternlieb, D. E. Cox, J. H. Brewer, R. Kadono, J. R. Kempton, and A. W. Sleight, "Absence of magnetic order in (Ba, K)BiO_3," Nature **335**(6186), 151–152 (1988).
[9]A. Kussmaul, E. S. Hellman, E. H. Hartford, Jr, and P. M. Tedrow, "Superconductor-insulator-superconductor tunneling in $Ba_{1-x}K_xBiO_3$ grain boundaries," Appl. Phys. Lett. **63**(20), 2824–2826 (1993).
[10]L. Fu and C. L. Kane, "Superconducting proximity effect and Majorana fermions at the surface of a topological insulator," Phys. Rev. Lett. **100**(9), 096407 (2008).
[11]M. Brahlek, L. Zhang, C. Eaton, H. T. Zhang, and R. Engel-Herbert, "Accessing a growth window for $SrVO_3$ thin films," Appl. Phys. Lett. **107**(14), 143108 (2015).
[12]B. Jalan, P. Moetakef, and S. Stemmer, "Molecular beam epitaxy of $SrTiO_3$ with a growth window," Appl. Phys. Lett. **95**(3), 032906 (2009).
[13]Y. Matsubara, K. S. Takahashi, Y. Tokura, and M. Kawasaki, "Single-crystalline $BaTiO_3$ films grown by gas-source molecular beam epitaxy," Appl. Phys. Express **7**(12), 125502 (2014).
[14]R. L. Bouwmeester, K. de Hond, N. Gauquelin, J. Verbeeck, G. Koster, and A. Brinkman, "Stabilization of the perovskite phase in the Y–Bi–O system by using a $BaBiO_3$ buffer layer," Phys. Status Solidi RRL **13**(7), 1800679 (2019).
[15]M. Zapf, M. Stübinger, L. Jin, M. Kamp, F. Pfaff, A. Lubk, and R. Claessen, "Domain matching epitaxy of $BaBiO_3$ on $SrTiO_3$ with structurally modified interface," Appl. Phys. Lett. **112**(14), 141601 (2018).
[16]R. Hu, A. E. Lee, H. W. Chan, and C. L. Pettiette-Hall, "Superconducting $Ba_{1-x}K_xBiO_3$ thin film by in-situ sputtering," IEEE Trans. Appl. Supercond. **3**(1), 1556–1558 (1993).
[17]E. S. Hellman, E. H. Hartford, and R. M. Fleming, "Molecular beam epitaxy of superconducting (Rb,Ba)BiO_3," Appl. Phys. Lett. **55**(20), 2120–2122 (1989).
[18]M. G. Norton, E. S. Hellman, E. H. Hartford, Jr., and C. B. Carter, "Compositionally modulated nucleation and growth of barium bismuth oxide thin films on MgO," Phys. C **205**(3–4), 347–353 (1993).
[19]A. Gozar, G. Logvenov, V. Y. Butko, and I. Bozovic, "Surface structure analysis of atomically smooth $BaBiO_3$ films," Phys. Rev. B **75**(20), 201402 (2007).
[20]T. M. T. Makita and H. A. H. Abe, "Control of crystal orientation for $BaBiO_3$ thin film on $SrTiO_3$(100) substrate using BaO buffer layer," Jpn. J. Appl. Phys. **36**(2A), L96 (1997).
[21]M. Iyori, S. Suzuki, K. Yamano, H. Suzuki, K. Takahashi, and Y. Yoshisato, "Preparation of $BaBiO_3$ thin films using an oxygen radical beam source," J. Cryst. Growth **150**, 1086–1089 (1995).
[22]C. Ferreyra, F. Marchini, P. Granell, F. Golmar, C. Albornoz, F. J. Williams, and D. Rubi, "Growth of (100)-highly textured $BaBiO_3$ thin films on silicon," Thin Solid Films **612**, 369–372 (2016).

[23]R. A. McKee, F. J. Walker, and M. F. Chisholm, "Crystalline oxides on silicon: The first five monolayers," Phys. Rev. Lett. **81**(14), 3014 (1998).
[24]C. Merckling, M. Korytov, U. Celano, M. H. M. Hsu, S. M. Neumayer, S. Jesse, and S. De Gendt, "Epitaxial growth and strain relaxation studies of $BaTiO_3$ and $BaTiO_3/SrTiO_3$ superlattices grown by MBE on $SrTiO_3$-buffered Si(001) substrate," J. Vac. Sci. Technol. A **37**(2), 021510 (2019).
[25]S. Franchi, "Molecular beam epitaxy: Fundamentals, historical background and future prospects," in *Molecular Beam Epitaxy* (Elsevier, 2013), pp. 1–46.
[26]T. H. Wang, P. C. Hsu, M. Korytov, J. Genoe, and C. Merckling, "Polarization control of epitaxial barium titanate ($BaTiO_3$) grown by pulsed-laser deposition on a MBE-$SrTiO_3$/Si(001) pseudo-substrate," J. Appl. Phys. **128**(10), 104104 (2020).
[27]T. H. Wang, R. Gehlhaar, T. Conard, P. Favia, J. Genoe, and C. Merckling, "Interfacial control of $SrTiO_3$/Si(001) epitaxy and its effect on physical and optical properties," J. Cryst. Growth **582**, 126524 (2022).
[28]W. Bennarndt, G. Boehm, and M. C. Amann, "Domains of molecular beam epitaxial growth of Ga(In)AsBi on GaAs and InP substrates," J. Cryst. Growth **436**, 56–61 (2016).
[29]S. Tixier, M. Adamcyk, T. Tiedje, S. Francoeur, A. Mascarenhas, P. Wei, and F. Schiettekatte, "Molecular beam epitaxy growth of $GaAs_{1-x}Bi_x$," Appl. Phys. Lett. **82**(14), 2245–2247 (2003).
[30]S. Migita, Y. Kasai, H. Ota, and S. Sakai, "Self-limiting process for the bismuth content in molecular beam epitaxial growth of $Bi_2Sr_2CuO_y$ thin films," Appl. Phys. Lett. **71**(25), 3712–3714 (1997).
[31]R. F. C. Farrow, "The stabilization of metastable phases by epitaxy," J. Vac. Sci. Technol. B **1**(2), 222–228 (1983).
[32]K. Bazaka, O. Baranov, U. Cvelbar, B. Podgornik, Y. Wang, S. Huang, and S. Xu, "Oxygen plasmas: A sharp chisel and handy trowel for nanofabrication," Nanoscale **10**(37), 17494–17511 (2018).
[33]E. S. Hellman and E. H. Hartford, "Adsorption controlled molecular beam epitaxy of rubidium barium bismuth oxide," J. Vac. Sci. Technol. B **8**(2), 332–335 (1990).
[34]C. D. Theis *et al.*, "Adsorption-controlled growth of $PbTiO_3$ by reactive molecular beam epitaxy," Thin Solid Films **325**(1–2), 107–114 (1998).
[35]R. Prasad, V. Venugopal, and D. D. Sood, "Vapour pressure of bismuth calculated from Mg + Bi and Pb + Bi alloys using a transpiration technique," J. Chem. Thermodyn. **9**(6), 593–601 (1977).
[36]T. Makita, M. Ogihara, F. Toda, and H. Abe, "Initial crystal growth stage of BRBO thin film," in *Advances in Superconductivity V* (Springer, Tokyo, 1993), pp. 919–922.
[37]M. B. Panish, "Molecular beam epitaxy," Science **208**(4446), 916–922 (1980).